PROCEEDINGS OF SCIENCE

Gamma-ray identification with Sb

P. M. Hansen,[a,b,c] **A. G. Mariazzi,**[a,b,*] **D. G. Melo,**[e] **L. Nellen**[d] **and I. D. Vergara Quispe**[a,b] **on behalf of the SWGO collaboration***

[a] *IFLP (CCT La Plata-CONICET-UNLP), Diagonal 113 y 63, La Plata, 1900, Argentina*
[b] *Departamento de Física, Facultad de Ciencias Exactas, Universidad Nacional de La Plata, C. C. 67, La Plata, 1900, Argentina*
[c] *Departamento de Ciencias Básicas, Facultad de Ingeniería, Universidad Nacional de La Plata, Calle 115 y 49, La Plata, 1900, Argentina*
[d] *Instituto de Ciencias Nucleares, UNAM, Circuito Exterior S/N, Coyoacán, 04510, Ciudad de México, Mexico*
[e] *ITeDA (CNEA - CONICET - UNSAM), CAC - CNEA, Av. Gral Paz 1499, San Martín, Buenos Aires, 1650, Argentina*
E-mail: pmhansen@iflp.unlp.edu.ar, vergarai@iflp.unlp.edu.ar, lnellen@nucleares.unam.mx, mariazzi@fisica.unlp.edu.ar, diego.melo@iteda.cnea.gov.ar

Gamma-ray observatories must efficiently distinguish gamma-ray-induced showers from the abundant background of hadronic showers. The shape of the lateral signal distribution offers crucial information for this task. S_b is a key observable that characterizes the shape of the lateral signal distribution. It is computed using the signal and position of each triggered detector, along with a free parameter, b. This work investigates the potential of S_b as a robust discriminator for gamma-ray identification in triangular grid arrays with varying detector densities. The behavior of the free parameter b was studied as a function of both the zenith angle and the shower size. A parametrization of b is provided for use in S_b on an event-by-event basis. This parametrization yields improvements in both merit and quality factors for gamma / hadron discrimination, demonstrating that S_b is a powerful separator for next-generation ground-based gamma-ray observatories such as SWGO.

39th International Cosmic Ray Conference (ICRC2025)
15–24 July 2025
Geneva, Switzerland

*Full list of authors available at: https://www.swgo.org/SWGOWiki/lib/exe/fetch.php?media=wiki:the_swgo_collaboration.
*Speaker

PoS(ICRC2025)748

1. Introduction

Gamma rays with energies above 100 GeV produced in astrophysical environments cannot be directly detected due to their extremely low flux at Earth. Instead, they are observed indirectly by reconstructing the extensive air showers (EAS) they produce upon interaction with the Earth's atmosphere. These showers generate cascades of secondary particles that can be sampled by ground-based observatories over large detection areas. While satellite-based instruments have provided crucial observations at lower energies (from MeV to a few tens of GeV), their limited effective area makes them inefficient at very-high-energy (VHE) ranges. Thus, ground-based detection becomes essential for studying the most energetic gamma-ray phenomena in the universe.

The detection of VHE gamma rays from the ground has opened an unprecedented window to explore extreme astrophysical processes and probe fundamental physics. It contributes significantly to multi-messenger astronomy, complementing neutrino, gravitational wave, and cosmic ray observations by offering insight into particle acceleration mechanisms in sources such as pulsar wind nebulae, supernova remnants, and active galactic nuclei.

To fully exploit this potential, it is essential to develop robust strategies for distinguishing gamma-ray-induced events from the overwhelming background of hadronic cosmic rays. This challenge is particularly relevant for large-area, wide-field-of-view experiments such as the *Southern Wide-field Gamma-ray Observatory*[1] (SWGO)[1], which is designed to provide continuous coverage of the southern sky and study transient and diffuse sources in the tens of TeV to PeV energy range.

Gamma/hadron (g/h) separation has traditionally relied on observables sensitive to the muonic content and morphology of the air showers. Several simple yet effective parameters have been successfully employed in previous experiments. For instance, the *compactness* parameter, introduced by the Milagro observatory [2], compares the largest PMT signal detected far from the reconstructed shower core to the number of triggered PMTs, exploiting the lower muon content in gamma showers. The HAWC experiment further developed this idea by implementing not only *compactness*, but also *PINCness* [3], which characterizes the smoothness of the lateral signal distribution. These parameters have proven robust and computationally efficient for real-time gamma/hadron separation.

Along this line, other discriminators have also been proposed, including methods based on the identification of muons at the station level [4], the azimuthal non-uniformity of particle distributions in concentric rings [5, 6], and full-image-based approaches using machine learning techniques [7].

Among these methods, the S_b parameter has proven to be an effective observable for composition studies and photon searches at ultra-high energies, particularly within the context of the Pierre Auger Observatory. There, it has been used to discriminate between proton and iron primaries [8], as well as between photons and hadrons [9, 10]. These studies exploit the lateral distribution of the signal in water Cherenkov detectors and the observable's sensitivity to shower development and muon content.

In this work, we extend the application of S_b to the energy and array conditions relevant for SWGO. Our analysis uses simulations of gamma- and proton-induced showers processed through the official SWGO software framework, which includes a realistic detector description and event

[1] https://www.swgo.org/SWGOWiki/doku.php

processing chain. Although this study is tailored to SWGO, the formulation of S_b remains broadly applicable to other ground-based gamma-ray experiments with similar detection principles.

We present the performance of S_b as a function of energy, zenith angle, and the number of triggered stations, highlighting its discrimination power through the evaluation of the Q-factor and the Merit Factor. The results demonstrate that S_b provides strong separation between gamma- and hadron-induced showers, making it a practical and effective tool for gamma/hadron discrimination in SWGO and future observatories.

2. SWGO Detector

The Southern Wide-field Gamma-ray Observatory (SWGO) is a ground-based gamma-ray detector designed to operate with a wide field of view and a high duty cycle. It is planned to be installed at the Atacama Astronomical Park in Chile, at an altitude of approximately 4.770 m.a.s.l. The observatory aims to detect primary particles in the energy range from 100 GeV up to the PeV scale [1].

At the current stage of the project, several candidate array configurations have been proposed. Among them, the D8 layout has been adopted as the reference design. It consists of water Cherenkov detector stations, each with a tank radius of 2.6 m, distributed across three concentric zones of progressively lower detector density with increasing distance from the array center.

The innermost zone extends to a radius of 156 m and comprises 2.587 detector stations, with a fill factor of $FF = 70\%$. The fill factor quantifies the fraction of the area effectively covered by detectors within each zone. The intermediate zone extends to 400 m and includes 792 stations ($FF = 4\%$), while the outermost zone, characterized by the lowest density ($FF = 1.7\%$), consists of 384 stations, as shown in Figure 1 (top-left).

Each station will be equipped with two photomultiplier tubes (PMTs): one positioned to observe the top of the tank, optimized for detecting the electromagnetic component of air showers, and another placed to view the bottom of the tank, enhancing sensitivity to the muonic component. This dual-PMT configuration is intended to improve the particle identification capabilities of the array.

The use of a density gradient in the array design serves to optimize performance across a broad energy range. The dense core enhances sensitivity to lower-energy showers, while the more sparsely instrumented outer regions extend the effective collection area for high-energy events, thereby maximizing the scientific reach of the observatory.

3. S_b Observable

The S_b observable was proposed and studied for gamma/hadron separation in the ultra-high-energy (UHE) regime [8, 9], using uniform arrays such as square and triangular grids. In the case of triangular layouts, station separations ranging from 500 m to 2000 m were considered. This observable has been successfully applied in composition studies at the Pierre Auger Observatory [11].

S_b captures the combined influence of the muonic and electromagnetic components on the lateral distribution function of air showers, which varies with the primary particle type for a given

energy. It is defined as:

$$S_b = \sum_{i=1}^{N} \left[S_i \times \left(\frac{r_i}{r_0} \right)^b \right], \tag{1}$$

where the sum runs over all triggered stations, S_i is the signal recorded at station i, r_i is its distance to the shower axis, r_0 is a reference distance, and b is a free parameter that can be tuned to enhance the separation power of the observable.

In a previous study, we proposed adapting the S_b observable to the SWGO array, which features zones of varying detector density [12]. In that work, we considered a simplified layout with two distinct density regions, showing that the non-uniformity affects the relative contribution of stations to the observable. To compensate for this, a weight factor w_i is applied to each station, defined as the inverse of the fill factor in the zone where it is located. For SWGO, the signal from the PMT at the top of the tank—primarily sensitive to the electromagnetic component—is used in the calculation of S_b:

$$S_b = \sum_{i=1}^{N} \left[S_i \times \left(\frac{r_i}{r_0} \right)^b \times w_i \right].$$

The reference distance adopted is $r_0 = 1000$ m, selected to keep the values of $(r_i/r_0)^b$ within a reasonable numerical range across the array.

In contrast to our previous analysis [12], where a fixed value of b was independently optimized in each bin of zenith angle and shower size, in this work we parametrize b as a continuous function of these two variables. The functional form was obtained by fitting the values of b that maximize the merit factor in each bin, revealing a linear dependence on the shower size within each zenith angle interval. Linear fits were performed for each zenith bin, resulting in a smooth parametrization of $b(\theta, \text{shower size})$ that can be applied on an event-by-event basis. This approach yields an improved merit factor compared to our earlier results [12].

4. Analysis and results

In our analysis, we simulated proton- and gamma-induced air showers using the CORSIKA Monte Carlo simulation program [13]. The detector response was modeled with the simulation and reconstruction framework developed by the SWGO Collaboration, based on the code originally implemented by the HAWC Collaboration. The simulation library follows an E^{-2} energy spectrum to ensure an even computational load across energy decades.

To evaluate the discrimination power of the S_b observable, we grouped events according to the $nHit_{up}^{(s)}$ variable. This parameter represents the total number of upward-facing PMTs triggered in an event, weighted by the same factor w_i used in the definition of S_b. This scaling ensures a uniform treatment of shower size and allows for meaningful comparisons across the full detector geometry.

The dataset was divided into eight intervals of $nHit_{up}^{(s)}$: (1000–2000), (2000–3000), (3000–4000), (4000–5000), (5000–6000), (6000–8000), (8000–11000), and (11000–15000). These intervals were selected to provide sufficient statistics within each energy range. As the flux of primary particles falls with energy, the bins corresponding to higher energies are broader to compensate for the lower number of events.

Additionally, events were binned in zenith angle using the following four intervals: 0°–22°, 22°–31°, 31°–38°, and 38°–45°. These bins were chosen to ensure uniform coverage in solid angle, allowing for a systematic analysis of the dependence of S_b on the angle of incidence.

To assess the discrimination power of the S_b observable, we computed the merit factor and the Q factor, defined respectively as:

$$MF = \frac{\mu_\gamma - \mu_p}{\sqrt{\sigma_\gamma^2 + \sigma_p^2}} \tag{2}$$

where μ and σ are the mean and the standard deviation of the S_b distributions; the subscripts γ and p refer to gamma and proton primaries. The Q factor is defined as:

$$Q = \frac{\epsilon_\gamma}{\sqrt{\epsilon_p}} \tag{3}$$

where ϵ_γ is the fraction of gamma-ray events retained after a selection cut, and ϵ_p is the fraction of proton events retained under the same cut.

These metrics were used to evaluate the separation power of the observable S_b across different values of the exponent b. For each combination of zenith angle and $nHit_{up}^{(s)}$ interval, the merit factor was calculated as a function of b, and the value that maximized the separation between gamma and proton showers was selected.

As an illustrative example, we show in figure 1(bottom) the results for the bin defined by zenith angles between 31° and 38°, and $nHit_{up}^{(s)}$ values between 8000 and 11000. This bin corresponds approximately to an average primary particle energy of 31.6 TeV. The top panel displays the merit factor as a function of b, indicating that the optimal value is $b = 1.5$, which yields a merit factor of 1.70. The bottom right panel of Figure 1 shows the distribution of S_b for this optimal b, displaying gamma-induced showers (blue) and proton-induced ones (red). The vertical line marks the median of the gamma distribution, used to estimate contamination at 50% efficiency. In this case, the median S_b is 3006.35, and the corresponding quality factor is 6.3. Once the optimal value of b was determined for each $nHit_{up}^{(s)}$ bin within each zenith angle interval, a linear dependence of b on $nHit_{up}^{(s)}$ was observed *within each zenith angle bin*. For each of these zenith angle bins, a linear fit was performed separately.

The resulting slopes showed a tendency to remain approximately constant with respect to $\sec(\theta)$. Based on this observation, the slope was recalculated using all zenith angle intervals combined, resulting in a value of $m = (9.64 \pm 0.66) \times 10^{-5}$. This fixed slope was then used to refit each bin individually in order to extract the corresponding intercepts consistently across all zenith angles.

The resulting intercepts were analyzed as a function of $\sec(\theta)$. Two approaches were tested: fitting the intercepts with a linear function, and approximating them by a constant. Since both methods produced similar results and the constant model is simpler to implement, we adopted the constant approximation, yielding a value of 0.52 ± 0.01. As a result, the parameter b can be expressed as a linear function of $nHit_{up}^{(s)}$, independent of the zenith angle:

$$b(nHit_{up}^{(s)}) = (9.64 \pm 0.66) \times 10^{-5} \cdot nHit_{up}^{(s)} + 0.52 \pm 0.01 \tag{4}$$

A summary of all results across the different zenith angle intervals is presented in Table 1. The first column in the table shows the range of $nHit_{up}^{(s)}$, the second column displays the merit factor

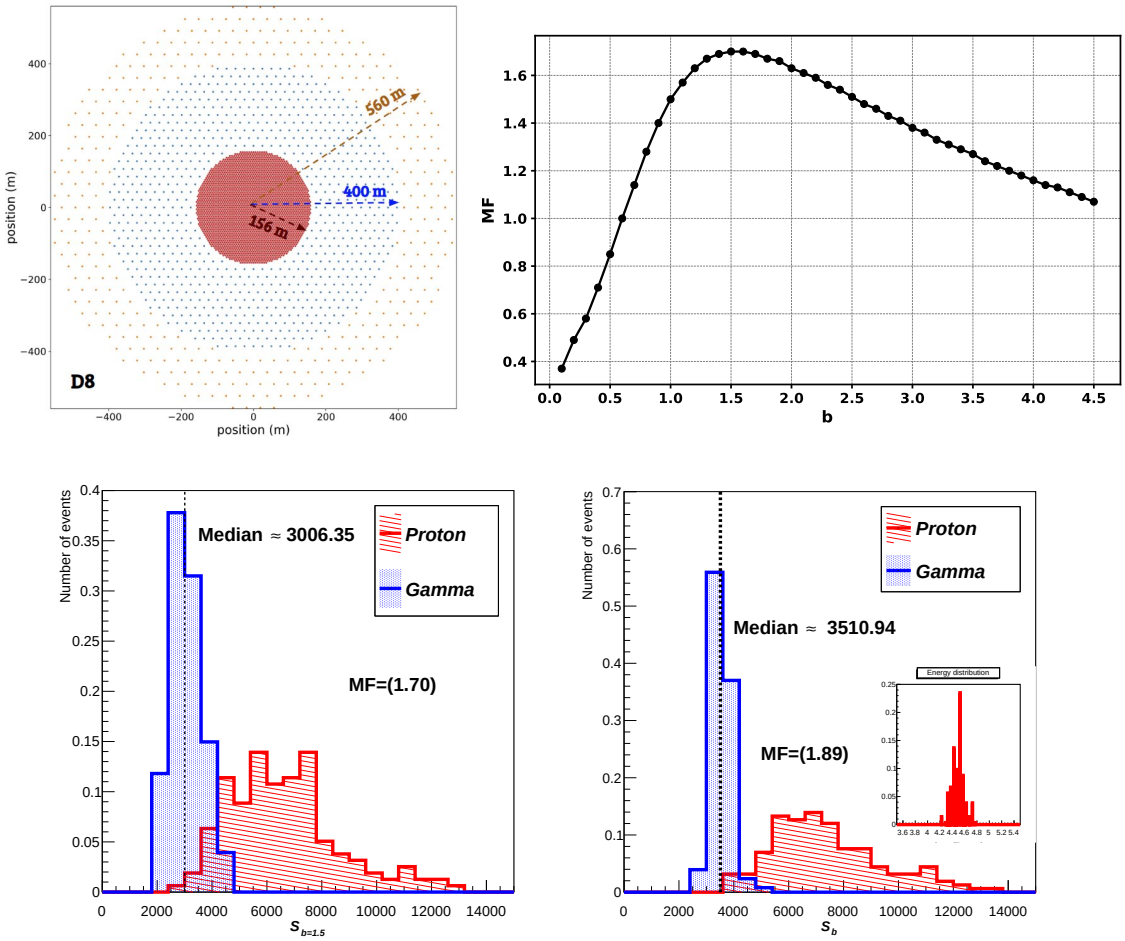

Figure 1: Top left: Layout of the SWGO detector array for configuration D8. **Top right:** Merit factor as a function of the parameter b. **Bottom left:** Distribution of S_b for events with zenith angles between 31° and 38° and $nHit_{up}^{(s)}$ between 8000 and 11000, using a fixed value $b = 1.5$. **Bottom right:** Same distribution using the parametrized $b(nHit_{up}^{(s)})$. The corresponding average reconstructed energy is approximately 31.6 TeV.

(MF) obtained using the optimal value of b determined individually for each bin, and the third column presents the MF computed using the parametrized function of $b(nHit_{up}^{(s)})$, as described in the previous section.

The corresponding Q factors are shown in the last two columns. In most cases, the values improve with the parametrization; however, the extent of this improvement cannot always be quantified, particularly when the Q factor is undefined. These undefined values result from insufficient statistics in the proton background. Nonetheless, the associated MF values indicate good separation power. For this reason, our analysis relies primarily on the merit factor, which remains well-defined even in low-statistics bins.

These tables show that, in most zenith angle intervals, the merit factor tends to increase with increasing $nHit_{up}^{(s)}$. As an illustrative example, we again show the result for the bin with zenith angles between 31° and 38°, and $nHit_{up}^{(s)}$ values between 8000 and 11000, but this time using the value of b given by the functional form described earlier. In this same figure, we show the primary

energy distribution corresponding to an average of 31.6 TeV for this bin (see Figure 1 bottom right).

A comparison between the values obtained using a constant b and those using the functional dependence reveals an improvement in the discrimination power. This demonstrates not only the benefit of parameterizing b as a function of shower size, but also reinforces the strong overall separation performance of the S_b observable.

$nHit_{up}$ range (min - max)	$b_{optimum}$ MF	$b_{optimum}(nHit_{up}^{(s)})$ MF	Q b_{opt}	Q $b(nHit_{up}^{(s)})$
Zenith angle: 0° – 22.1°				
(1000 – 2000)	0.94	0.84	3.04	2.92
(2000 – 3000)	1.10	1.13	(3.28-3.74)	4.18
(3000 – 4000)	1.21	1.24	(3.75-3.96)	3.75
(4000 – 5000)	1.30	1.26	8.80	undef
(5000 – 6000)	1.36	1.42	7.39	undef
(6000 – 8000)	1.21	1.36	(3.66-4.72)	undef
(8000 – 11000)	1.56	1.83	undef	undef
(11000 – 15000)	1.69	1.88	undef	undef
Zenith angle: 22.1° – 31.4°				
(1000 – 2000)	0.91	0.93	2.35	2.84
(2000 – 3000)	1.25	1.27	4.02	4.34
(3000 – 4000)	1.22	1.25	3.91	4.52
(4000 – 5000)	1.43	1.43	6.04	8.54
(5000 – 6000)	1.48	1.49	6.92	6.92
(6000 – 8000)	1.47	1.50	7.48	undef
(8000 – 11000)	1.82	1.99	6.55	undef
(11000 – 15000)	1.53	1.61	undef	undef
Zenith angle: 31.4° – 38.7°				
(1000 – 2000)	0.95	0.99	2.67	3.07
(2000 – 3000)	1.11	1.14	(2.94-3.10)	4.27
(3000 – 4000)	1.52	1.59	9.84	undef
(4000 – 5000)	1.37	1.37	undef	undef
(5000 – 6000)	1.45	1.45	6.18	6.18
(6000 – 8000)	1.68	1.73	6.51	undef
(8000 – 11000)	1.70	1.89	6.28	undef
(11000 – 15000)	1.83	2.04	undef	undef
Zenith angle: 38.7° – 45°				
(1000 – 2000)	0.94	0.96	(2.83-2.95)	3.67
(2000 – 3000)	1.20	1.25	4.78	6.17
(3000 – 4000)	1.22	1.27	8.15	8.15
(4000 – 5000)	1.43	1.42	undef	undef
(5000 – 6000)	1.82	1.91	undef	undef
(6000 – 8000)	1.70	1.67	undef	undef
(8000 – 11000)	1.33	1.36	4.94	undef
(11000 – 15000)	1.81	1.74	undef	undef

Table 1: Discrimination power of the S_b observable. Shown are the $nHit_{up}^{s}$ ranges, the merit factor (MF), and the quality factor (Q) at 50% efficiency, for each zenith angle bin. Results are given for both the optimal fixed b in each bin and the event-wise parametrized $b(nHit_{up}^{(s)})$.

5. Conclusion

In this work, we evaluated the performance of the S_b observable for gamma/hadron discrimination in the SWGO detector, using the D8 configuration. We analyzed its dependence on shower size and zenith angle. By scanning a range of values for the exponent b, we determined the optimal values that maximize the merit factor for each bin in $nHit_{up}^{(s)}$ and zenith angle.

We observed a systematic dependence of the optimal b on the shower size, which we quantified through a linear parametrization. This parametrization significantly simplifies the implementation of the observable without sacrificing performance. Moreover, we found that the slope of this dependence is consistent across zenith angle intervals, allowing for a unique, zenith-independent formulation.

Incorporating a scaling factor to account for the different station densities in the central, intermediate, and outer regions of the array proved essential for maintaining the robustness of the S_b calculation across the entire detector.

Comparative studies using this parametrized form of b show that it reproduces the discrimination power obtained with bin-wise optimization and, in many cases, leads to an improved merit factor. The final expression for b as a function of $nHit_{up}^{(s)}$ enables a robust and simple implementation across the full range of energy and zenith angles covered by SWGO. These results demonstrate the strong separation capabilities of the S_b observable and support its use in future analyses aiming at gamma/hadron discrimination in wide-field water Cherenkov observatories.

Acknowledgments

The SWGO Collaboration acknowledges the support from the agencies and organizations listed here https://www.swgo.org/SWGOWiki/doku.php?id=acknowledgements and from grants listed here https://www.overleaf.com/project/64a843bd0110a0b0d21052e1

References

[1] SWGO Collaboration, *Science Prospects for the Southern Wide-field Gamma-ray Observatory:SWGO*, doi:10.48550/arXiv.2506.01786

[2] A. J. Smith *et al.*, *The Milagro Gamma-Ray Observatory: Gamma-ray Detection via Water Cherenkov Techniques*, *Nucl. Instrum. Meth. A* **553** (2005) 325–331, doi:10.1016/j.nima.2005.07.085.

[3] T. Capistrán *et al.*, *Gamma/hadron separation parameters for the HAWC Observatory*, Proc. 35th International Cosmic Ray Conference (ICRC2017), PoS(ICRC2017)745 (2017).

[4] R. Conceição *et al.*, $P_{\gamma h}^{\alpha}$: *A new variable for γ/h discrimination in large gamma-ray ground arrays*, Phys. Lett. B, 827, 136969, 2022.

[5] R. Conceição *et al.*, *Gamma/hadron discrimination at high energies through the azimuthal fluctuations of air shower particle distributions at the ground*, JCAP, 10, 086, 2022.

[6] R. Conceição *et al.*, *The gamma/hadron discriminator LCm in realistic air shower array experiments*, Eur. Phys. J. C, 83, 932, 2023.

[7] R. Conceição *et al.*, *Discriminating sub-TeV gamma and hadron-induced showers through their footprints*, Phys. Rev. D, 111, 043047, 2025.

[8] G. Ros *et al.*, *A new composition-sensitive parameter for ultra-high energy cosmic rays*, Astropart. Phys., 35, 140-151, 2011.

[9] G. Ros *et al.*, *Improving photon-hadron discrimination based on cosmic ray surface detector data*, Astropart. Phys., 47, 10-17, 2013.

[10] The Pierre Auger Collaboration, *Search for photons with energies above* 10^{18} *eV using the hybrid detector of the Pierre Auger Observatory*, JCAP , 2017, 009, 2017.

[11] Pierre Auger Collaboration, *A Search for Photons with Energies Above* 2×10^{17} *eV Using Hybrid Data from the Low- Energy Extensions of the Pierre Auger Observatory*, The Astrophysical Journal, 933, 125, 2022.

[12] I. D. Vergara Quispe *et al.* for the SWGO collaboration *S_b for gamma/hadron separation in SWGO*, PoS(ICRC2023)952, 2023.

[13] D. Heck *et al.*, *CORSIKA: a Monte Carlo code to simulate extensive air showers*, Forschungszentrum und Universität Karlsruhe, Karlsruhe (FZKA-6019), 1998, https://pos.sissa.it/301/745.